Article

Not peer-reviewed version

Optimization of Basketball Shoe Design Concepts Based on Geomechanics and Neural Networks

Wencan Guan *

Posted Date: 21 July 2025

doi: 10.20944/preprints202507.1669.v1

Keywords: Numerical analysis; Geomechanics; Neural networks; Sports science; Elastic mechanics

 doi:10.20944/preprints202507.1669.v1

Article

Optimization of Basketball Shoe Design Concepts Based on Geomechanics and Neural Networks

You-Liang Chen and Wen-Can Guan *

University of shanghai for science and technology

* Correspondence：guanwencan123@outlook.com

Abstract

This study examines the optimization and upgrading of basketball shoes from the perspective of engineering mechanics, including the introduction of the concept of soil mechanics in the reinforcement of the midsole of basketball shoes. This method has been found to effectively reduce the deformation of the upper and the torsion of the sole during sudden stops in basketball, while enhancing the overall stability of basketball shoes. Furthermore, the plastic surface is fitted using a neural network and deep learning to obtain the shoe reinforcement surface. This method allows for the improvement of both the service life of the basketball shoes and the athletic performance of the athletes without the necessity of upgrading the upper and sole materials.

Keywords: Numerical analysis; Geomechanics; Neural networks; Sports science; Elastic mechanics

1. Introduction

The design of sports footwear has seen advances in segmented technology for athletic health, yet there remains a deficiency in the optimization of engineering mechanics for footwear [1]. Due to varying intensities of physical activities, most designs primarily focus on optimizing the material properties of the upper fabric. Nike often employs Flyknit technology for their shoe uppers. Flyknit is a technique that weaves fibers to create shoe uppers, using a special knitting method to form structures of varying densities and strengths to meet the needs of different areas. This technology enables precise weaving of fibers into the required shapes and structures of the upper, achieving an optimal balance of lightness, breathability, and comfort. Adidas commonly uses Primeknit technology for their shoe uppers, a weaving technique similar to Flyknit, which crafts synthetic fibers into the shoe upper. This technique offers lightweight, breathable, and comfortable uppers that can be customized to fit an athlete's foot shape, providing enhanced fit and support [2]. Despite the advantages of lightweight, breathability, and comfort brought by Nike and Adidas's upper technologies, challenges in durability, support, and maintenance costs persist. This paper introduces a novel design approach from an engineering mechanics perspective, applying the generalized nonlinear criterion from soil mechanics in civil engineering, combined with the theoretical framework of the Cambridge mode. Utilizing the three-dimensional stress Mohr's circle and plane problem solutions in elasticity mechanics, incorporating the Airy stress function solutions, and blending sports science design principles, this study employs Ansys software for static structure modeling and analysis. The analysis investigates the mechanical behaviors of basketball shoes during abrupt stopping motions, using mechanical analysis and theoretical deduction to enhance the performance and lifespan of basketball shoes. By exploring different approaches, this study aims to revolutionize the technology, reduce future costs, and enhance performance [3]. Using commercially available basketball shoes as reference templates, this research optimizes technical bottlenecks based on existing studies. Employing the above theoretical framework, the study identifies the causes of upper damage through fundamental elasticity mechanics, maps out stress spaces and stress surfaces, and conducts finite element numerical analysis on abrupt stopping motions in basketball. It then theoretically optimizes existing yield surfaces and strength criteria in the material constitutive

 doi:10.20944/preprints202507.1669.v1

relationship field, and validates the results with comparative analysis before and after the improvements[4].

2. Analysis and Comparison of Strength of Basketball Shoe Upper Fabrics

Based on the manufacturing processes of athletic shoes, they can be classified into four categories: cold adhesive sports shoes, hot vulcanized adhesive shoes, injection and casting shoes, and molded shoes. The manufacturing process is related to the way the upper and sole of the shoe are combined. The formation of the upper by new molding processes and the use of new materials may be constrained by the low melting points of some materials, which affect the choice of how they are combined with the sole. Currently, raw materials used for shoe uppers are mainly filament fibers, which can be classified into three categories based on their functions: the first category serves as the main support, mostly using polyester low-elastic filaments, nylon low-elastic filaments, and high-elastic filaments; the second category serves for bonding and reinforcement, mainly including polyester hot melt filaments, nylon hot melt filaments, and polyester low-melting core filaments; the third category aims to enhance the elasticity of the shoe upper materials, including spandex bare filaments, polyester spandex-covered filaments, and nylon spandex-covered filaments. Research conducted by Yang Xi, Jiang, and Lu Zhiwen indicates that under the same raw materials, different weaving processes result in significant variations in the tensile stress-strain curves of fabrics with different organizational structures. Among them, the longitudinal fracture strength of the air layer organization is the best, and the transverse fracture stress of the air layer organization with 1 stitch flip per 1 stitch is the bes[1]. However, hole-type organizations have poor longitudinal fracture strength, so they should not be used extensively on the upper. Different coil structures such as moving coils, flipping coils, and gathering coils have different effects on fabric performance, so different organizational structures should be used in shoe upper design according to the requirements[2]. Although there is a rich variety of changes in the horizontal woven fabric organization, the specific impact of coil structures on mechanical performance still requires further research. Research results by Qin Ji [3] and Fang Fang show that during abrupt stop movements, the inertia of the human body causes slippage in the direction of motion, and loose wrapping provides poor stability for the foot in the shoe space, resulting in greater slippage and increased joint angles, while tighter wrapping provides better integration of the shoe with the foot, reducing slippage and decreasing joint angles, thus reducing the risk of sports injuries. Basketball shoes with integrated uppers mostly use knitted fabrics with good stretch and elastic recovery properties. Consequently, they are more prone to deformation under stress during abrupt stop movements, resulting in poorer control over foot slippage.

On the other hand, shoes with tongues mainly rely on shoelaces to adjust the wrapping degree. The stretchability of the upper is not as good as that of knitted uppers, so they undergo less deformation under stress and provide better stability for the foot within the shoe. Adjusting the wrapping degree of the upper can reduce the risk of knee and ankle injuries to a certain extent. Basketball shoes can be designed to create more ideal and personalized wrapping degree adjustment methods for users based on different needs, such as changing the traditional lacing method to an automatically adjustable lacing system according to the wearer's different occasions, thus achieving a balance between sports protection and comfort. Alternatively, new phase-change materials, such as polyurethane foam, can disperse impact through phase changes. When the shoe upper is subjected to excessive pressure or tension, the material hardens to stabilize the shape of the upper, thereby reducing the increase in shoe space.

During risky movements such as abrupt stops, efforts should be made to maintain the original wrapping degree to preserve the original sports protection function. Another material is D3O[4], which changes from fluid to foam structure after being subjected to impact, thereby reducing impact. The influence of sports shoes on athletes is also affected by individual differences, so further research is needed on the design of sports protection functions for sports shoes and the degree of individual impact on athletes.

 doi:10.20944/preprints202507.1669.v1

The above research indicates that during turning and abrupt stop movements, shoes are subjected to torsional and bending forces. These forces cause complex bending and shear stresses in the shoe material, especially at critical areas of the shoe, such as the junction of the sole and upper or the ankle support area. During player movement, the shoe upper may be subjected to tensile stress from foot movements, especially during jumping and turning. This tensile stress may cause stretching deformation of the shoe upper material, leading to tearing or rupture of the upper. Friction between the upper and the court surface during sports can cause wear. This wear may gradually weaken the surface of the upper material, making it susceptible to cracks or abrasions from other stresses.

Repetitive movements and stress may cause fatigue in the upper material, especially in critical areas such as the ankle support area. This fatigue may cause the upper material to lose its original strength and elasticity, ultimately leading to damage.

3. Theoretical Analysis and Optimization of Shoe Upper Elastic Mechanics

The basic equations of elastic mechanics include equilibrium differential equations.

$$\sigma_{ij,i}+F_j=0\left(\varrho\frac{\partial^2 u_j}{\partial t^2}\right) \tag{1}$$

In which $\sigma_{ij,i}$ represents the stress gradient term, F_j represents the body force term, and $\varrho\frac{\partial^2 u_j}{\partial t^2}$represents the acceleration term.

$$\sigma_{ij}=\lambda\varepsilon_{kk}\delta_{ij}+2G\varepsilon_{ij} \tag{2}$$

Where λandGare the Lamé constants. The state equation is controlled by the invariants of the stress tensor.

$$I_1=\sigma_x+\sigma_y+\sigma_z \tag{3}$$

$$I_2=\sigma_y\sigma_z+\sigma_x\sigma_z+\sigma_y\sigma_x-\tau_{yz}^2-\tau_{xz}^2-\tau_{xy}^2 \tag{4}$$

$$I_3=\begin{vmatrix}\sigma_x & \tau_{yx} & \tau_{zx}\\ \tau_{xy} & \sigma_y & \tau_{zy}\\ \tau_{xz} & \tau_{yz} & \sigma_z\end{vmatrix} \tag{5}$$

In the equation, σ represents normal stress, τ represents shear stress, andI represents the components of the stress invariants. The above control equation indicates that the acceptable state for the stressed object is when it is projected within the gray area of the three-dimensional stress Mohr's circle[5].

The results indicate that the shoe upper is susceptible to instantaneous torsional and shearing damage during movement, particularly at the seams connecting with the midsole, where instantaneous torsion and shear damage are likely to occur.

Assuming the microelement at the joint is a rectangle, with height h and width x, one end fixed, the upper surface subjected to a uniformly distributed pressure q, and the free end subjected to a concentrated force F and a couple M, solving for the stress components will identify the primary factors contributing to maximum damage. The solution is based on the physical interpretation of Airy's stress function.

The boundary conditions are as follows.

$$(U)_{y=\frac{h}{2}}=-\left(M+F_x+\frac{1}{2}qx^2\right) \tag{6}$$

$$\left(\frac{\partial U}{\partial y}\right)_{y=\frac{h}{2}}=0 \tag{7}$$

$$(U)_{y=-\frac{h}{2}}=0 \tag{8}$$

$$\left(\frac{\partial U}{\partial y}\right)_{y=-\frac{h}{2}}=0 \tag{9}$$

To satisfy the first stress boundary condition, the stress function is as follows.

$$U=f_0(y)+f_1(y)x+\frac{1}{2}f_2(y)x^2 \tag{10}$$

 doi:10.20944/preprints202507.1669.v1

Based on the boundary conditions, we have.

$$(f_0)_{y=\frac{h}{2}}=-M,(f_1)_{y=\frac{h}{2}}=-F \tag{11}$$

$$(f_2)_{y=\frac{h}{2}}=-q,\left(\frac{df_0}{dy}\right)_{y=\frac{h}{2}}=0 \tag{12}$$

$$\left(\frac{df_1}{dy}\right)_{y=\frac{h}{2}}=0,\left(\frac{df_2}{dy}\right)_{y=\frac{h}{2}}=0 \tag{13}$$

$$(f_0)_{y=-\frac{h}{2}}=0,(f_1)_{y=-\frac{h}{2}}=0 \tag{14}$$

$$(f_2)_{y=-\frac{h}{2}}=0,\left(\frac{df_0}{dy}\right)_{y=\frac{h}{2}}=0 \tag{15}$$

$$\left(\frac{df_1}{dy}\right)_{y=-\frac{h}{2}}=0,\left(\frac{df_2}{dy}\right)_{y=-\frac{h}{2}}=0 \tag{16}$$

The stress function is then.

$$U=f_0(y)+f_1(y)x+\frac{1}{2}f_2(y)x^2 \tag{17}$$

Substitute into Airy's stress function（10）.

$$\nabla^2\nabla^2U=\frac{\partial^4u}{\partial x^2}+2\frac{\partial^4u}{\partial x^2\partial y^2}+\frac{\partial^4U}{\partial y^4}=0 \tag{18}$$

The conditions it must satisfy are.

$$2\frac{d^2f_2}{dy^2}+\frac{d^4f_0}{dy^4}=0 \tag{19}$$

$$\frac{d^4f_1}{dy^4}=0 \tag{20}$$

$$\frac{d^4f_2}{dy^4}=0 \tag{21}$$

To find the general solution of the above equation, the boundary conditions can be used to determine the unknown constants.

$$f_0=-\frac{1}{2}M\left(1+3\frac{y}{h}-4\frac{y^3}{h^3}\right)-\frac{1}{80}qhy\left(1-\frac{4y^2}{h^2}\right)^2 \tag{22}$$

$$f_1=-\frac{1}{2}F\left(1+3\frac{y}{h}-4\frac{y^3}{h^3}\right) \tag{23}$$

$$f_2=-\frac{1}{2}q\left(1+3\frac{y}{h}-4\frac{y^3}{h^3}\right) \tag{24}$$

Substitute the coefficients into the stress function.

$$U=f_0(y)+f_1(y)x+\frac{1}{2}f_2(y)x^2 \tag{25}$$

This yields:

$$U=-\frac{1}{2}\left(M+Fx+\frac{1}{2}qx^2\right)\left(1+3\frac{y}{h}-4\frac{y^3}{h^3}\right)-\frac{1}{80}qhy\left(1-\frac{4y^2}{h^2}\right)^2 \tag{26}$$

(26)

Finally, the stress components are obtained as:

$$\sigma_x=\frac{12y}{h^3}\left(M+Fx+\frac{1}{2}qx^2\right)-q\left(\frac{4y^3}{h^3}-\frac{3y}{5h}\right) \tag{27}$$

$$\sigma_y=-\frac{1}{2}q\left(1+3\frac{y}{h}-\frac{4y^3}{h^3}\right) \tag{28}$$

$$\tau_{xy}=\frac{3}{2h}(F+qx)\left(1-\frac{4y^2}{h^2}\right) \tag{29}$$

From the above derivation of the mechanical analysis of material microelements during a basketball shoe's abrupt stopping action, the changes in the three principal stress components and the stress space surfaces are displayed using Matlab, as illustrated in the following figure.

 doi:10.20944/preprints202507.1669.v1

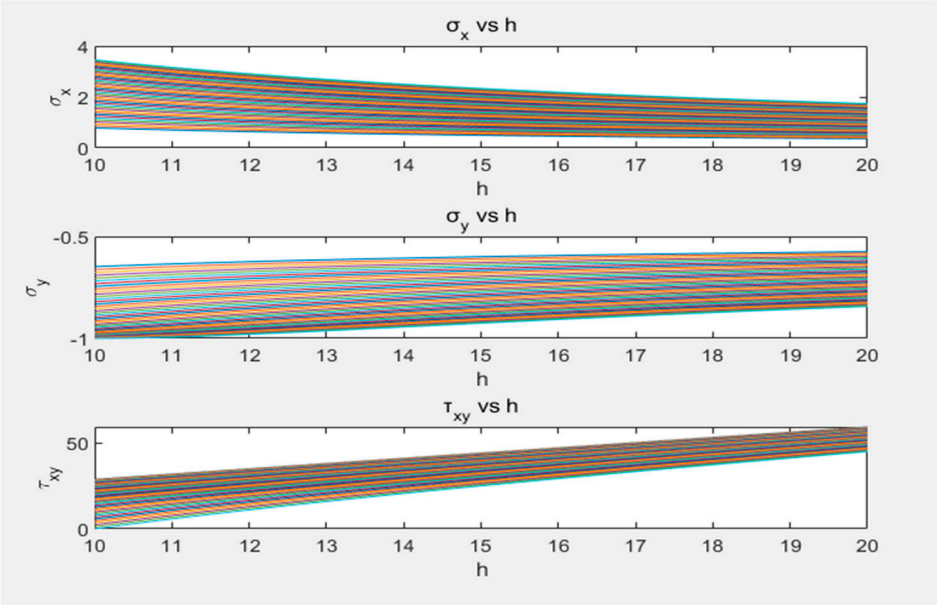

Figure 1. Schematic diagram of the plane of stress.

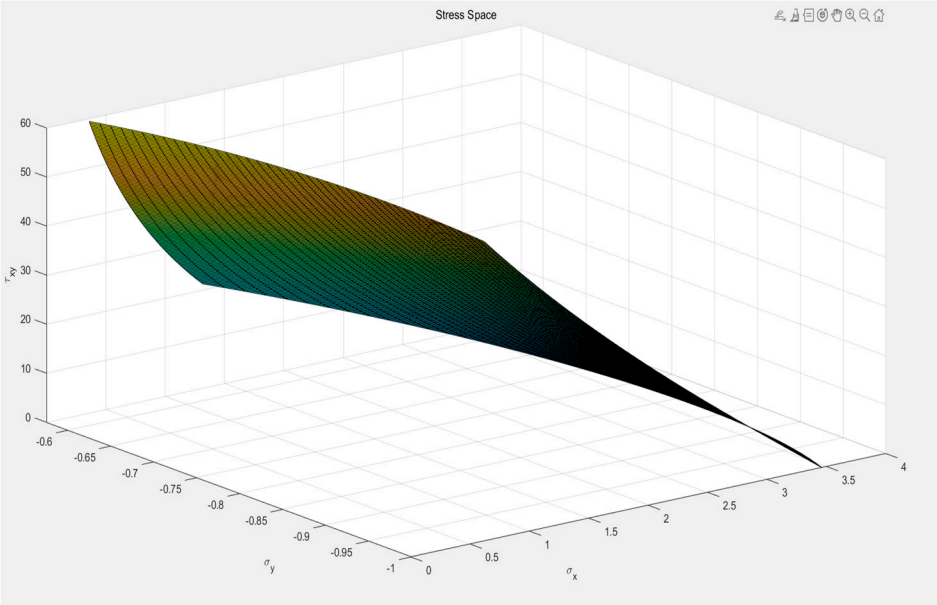

Figure 2. Stress spatial boundary surface.

The results indicate that the state surface in the stress space is in a waveform rising state. Based on this, the model is analyzed and optimized from the perspective of changes in the yield surface, and arguments are made. This is combined with the cyclic stress constitutive relationships from soil mechanics and the energy method of the Cam Clay model to analyze, optimize, and validate the model.

4. Numerical Analysis and Finite Element Simulation of Abrupt Stopping Actions in Basketball

Using Rhino software, the basketball shoe design is constructed and then imported into Ansys software. Through static structural analysis, the most unfavorable values of deformation, stress, and strain are obtained. Based on the analyses and comparisons in Chapter 4, the core concepts and ideas of this thesis are validated.

Starting with the original design in Rhino software, the model uses a typical commercial basketball shoe as a baseline. The design does not consider engineering mechanics optimization but

 doi:10.20944/preprints202507.1669.v1

focuses on factors related to motion protection. The design integrates wrap-around fit, comfort, and aesthetics, as illustrated in the figure.

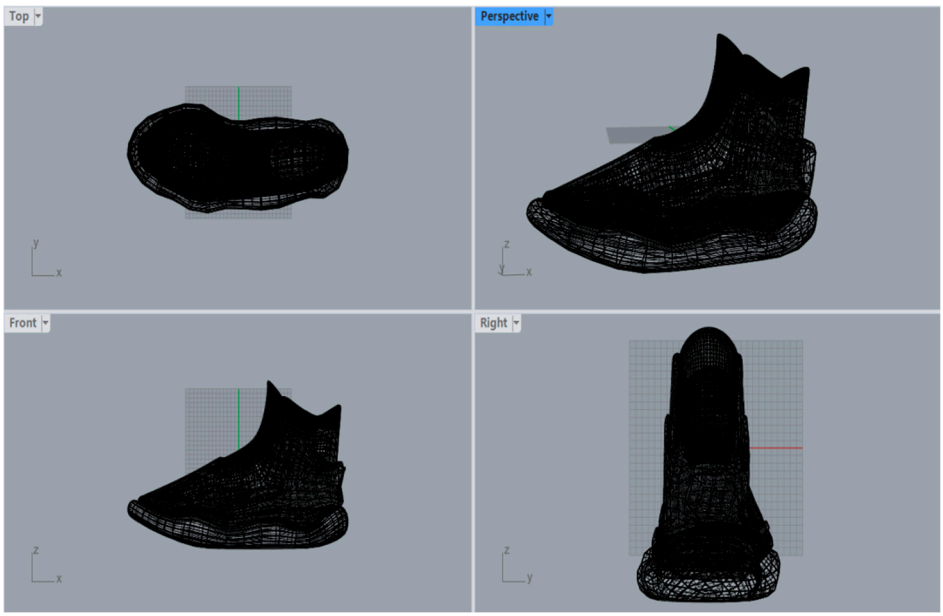

Figure 3. Original design sketch for basketball shoes.

Import the simplified model into Ansys, with the shoe upper using polyamide resin/nylon 66 as the material property, and the shoe sole using SAN foam (81 kg/m³) as the material. The figure illustrates the shoe body after mesh division.

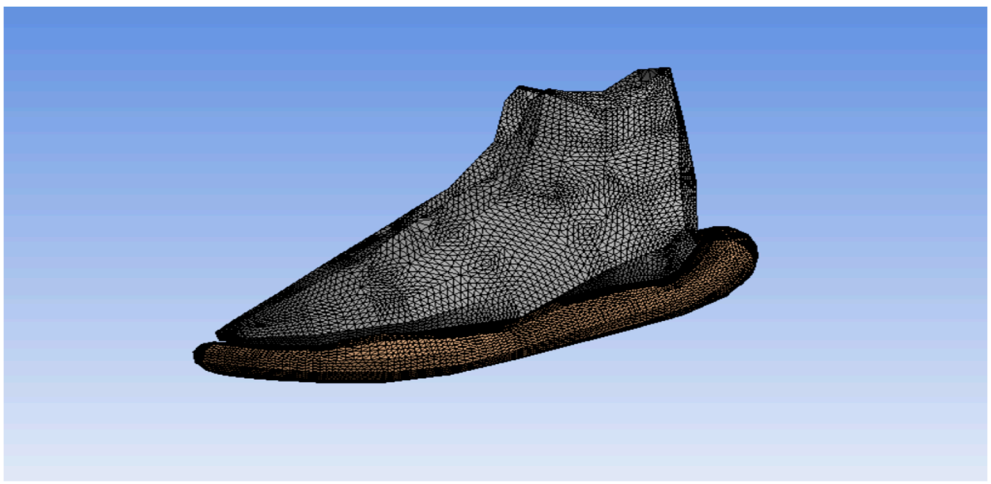

Figure 4. The shoe body is divided into a grid.

Conduct a static structural analysis to decompose the forces and torque involved in an abrupt stopping action. The force-bearing surface is located at the connection between the shoe's outer midsole and the upper. Assuming an adult male weighing 75 kg (approximately 150 pounds) and 175 cm tall, an average abrupt stopping action produces an acceleration of 6 meters per second squared, resulting in a force of 450 Newtons acting on the outer surface of the shoe and the contact surface of the midsole. At the same time, a clockwise torque of 45 Newton-meters is generated. The midsole provides elastic support and protection, while the full principal elements of the shoe sole provide fixed support. The midsole generates a positive linear pressure of 12 Newtons. This data is used as a reference for the analysis, as shown in the figure.

 doi:10.20944/preprints202507.1669.v1

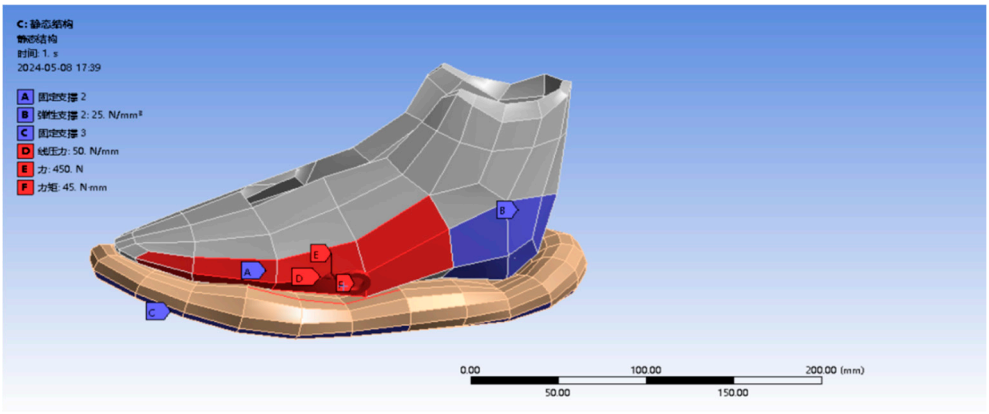

Figure 5. Load on shoes.

Based on the model test, the deformation, strain energy, total stress, and equivalent stress contour maps are obtained, as illustrated in the figure.

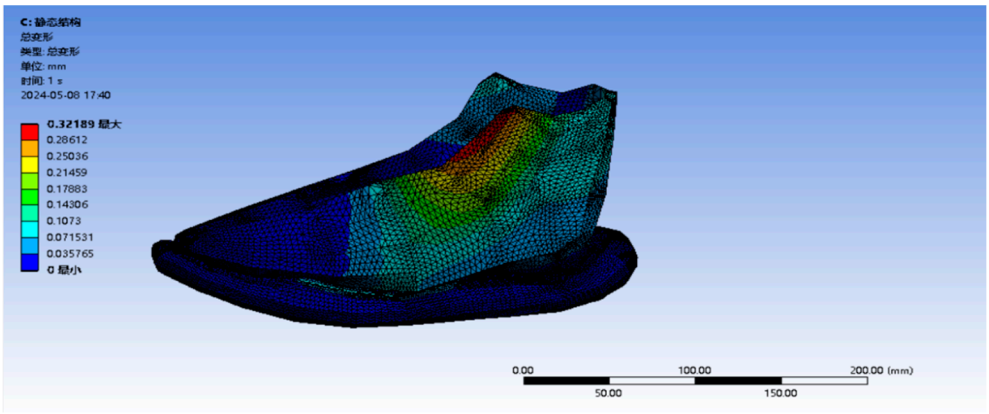

Figure 6. Total deformation of the shoe body.

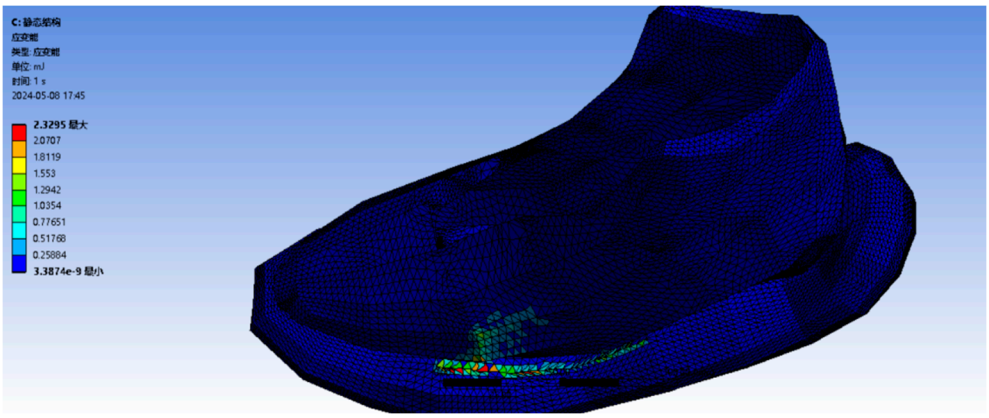

Figure 7. Strain energy diagram of the shoe body.

Abrupt stopping actions cause significant deformation and breakage at the connection between the shoe upper and the outer part of the sole. Additionally, due to ergonomics and sports science, significant deformation occurs at the ankle, which is extremely detrimental to athletic performance and poses a serious threat to the health of professional basketball players.

 doi:10.20944/preprints202507.1669.v1

5. Engineering Mechanics Optimization and Finite Element Simulation Verification

The research indicates that the most adverse factors under abrupt stopping actions in basketball shoes have been identified. Based on geotechnical engineering mechanics and incorporating the energy method of the Cambridge model, the contact design of basketball shoes is optimized without changing the materials, aiming to enhance their lifespan and safety.

The Cam Clay model includes the following formula:

$$dw^{p}=p d\varepsilon_{v}^{p}+q d\varepsilon_{d}^{p} \tag{30}$$

$$=p\sqrt{(d\varepsilon_{v}^{p})^{2}+\left(M d\varepsilon_{d}^{p}\right)^{2}} \tag{31}$$

$$D=\frac{d\varepsilon_{v}^{p}}{d\varepsilon_{d}^{p}}=\frac{M^{2}p^{2}-q^{2}}{2pq} \tag{32}$$

Where dw^{p} represents plastic work, $d\varepsilon_{v}^{p}$ and $d\varepsilon_{d}^{p}$ respectively denote the volumetric plastic strain and deviatoric plastic strain. p and q represent the mean normal stress and generalized shear stress, respectively, D is the dilatancy factor, and M is a coefficient. Solve for the plastic potential function [6].

$$g=q^{2}+M^{2}p^{2}-cp=0 \tag{33}$$

Where g represents the plastic potential function, and cis the hardening coefficient. According to the associated flow rule, the yield function is equal to the plastic potential function·

$$f=q^{2}+m^{2}p^{2}-cp=0 \tag{34}$$

Where f represents the yield function, and m is the mass.

At the critical state.

$$q=0,\ p=p_{x},d\varepsilon_{v}^{p}=0,e=e_{0} \tag{35}$$

Where e represents the porosity.

The solution is obtained as:

$$f=q^{2}+M^{2}p^{2}-M^{2}p_{x}p \tag{36}$$

From the v-p curve, the incremental elastoplastic constitutive relationship can be derived[7].

$$q^{2}+M^{2}p^{2}=M^{2}p^{2}\frac{P_{x}}{p} \tag{37}$$

After taking the logarithm and rearranging, the result is obtained as:

$$ln\left(1+\frac{q^{2}}{m^{2}p^{2}}\right)=ln\frac{p_{x}}{p} \tag{38}$$

Substitute $ln\,p_{x}$ into the original yield function to obtain:

$$f=\frac{\lambda-k}{1+e_{0}}ln\frac{P}{p_{0}}+\frac{\lambda-k}{1+e_{0}}\ln\left(1+\frac{q^{2}}{M^{2}p^{2}}\right)-\varepsilon_{v}^{p}=0 \tag{39}$$

Where λ is the shear dilatancy stress ratio, and k is the slope of the stress-strain relationship for the soil at the critical state.

By applying the consistency equation, utilizing the orthogonality condition, and assuming Drucker's coaxiality, the plastic potential function can be determined as:

$$g=\left(\frac{1}{2}p_{c}^{'}+\frac{\left[\left(p_{c}^{'}\right)^{2}+1\right]^{\frac{1}{2}}}{2}+\frac{1}{2}\right)M+\frac{q}{p}-c=0 \tag{40}$$

Thus, the yield surface can be plotted, as shown in the figure.

 doi:10.20944/preprints202507.1669.v1

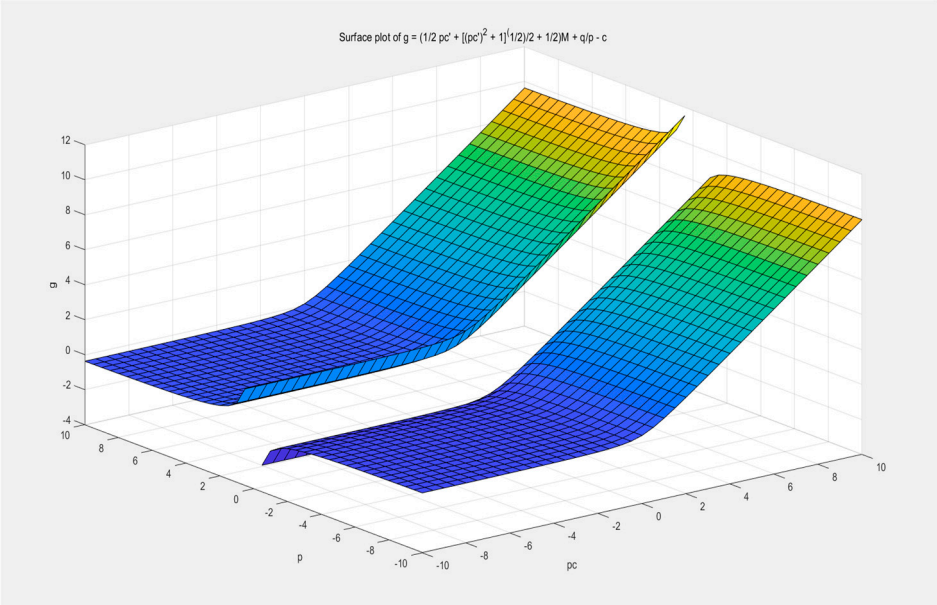

Figure 8. the yield surface.

6. Neural Network based yield surface fitting

The algorithm utilizing neural networks is based on the formula (27)(28)(29) ula, with the plastic potential energy surface equation (40) data to a mode.

Training Complex Neural Networks with the MATLAB Deep Learning Toolbox.Create a feedforward neural network with three layers of 20 neurons each. The input of the defined stress equation and plastic potential energy function into the training data is necessary for the prediction of the data and the fitting of the yield surface. The training algorithm used is Levenberg-Marquardt and the computational method is MEX.

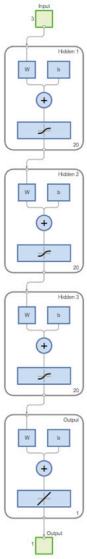

Figure 9. network diagram.

 doi:10.20944/preprints202507.1669.v1

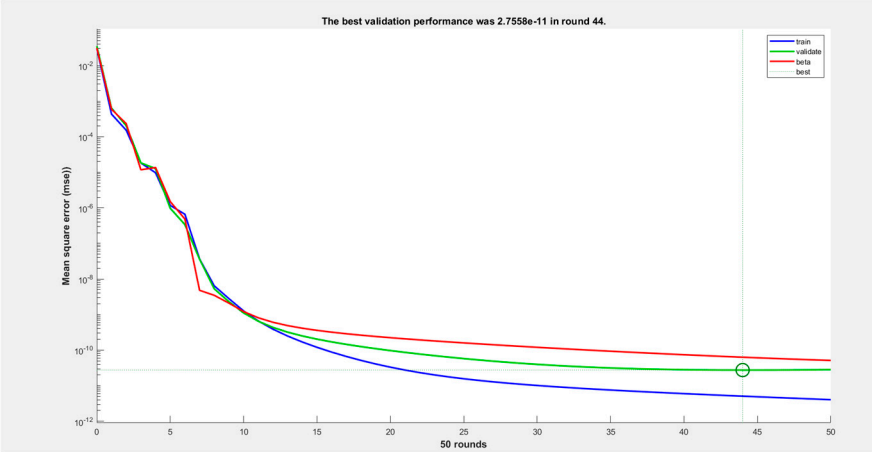

Figure 10. performance graph.

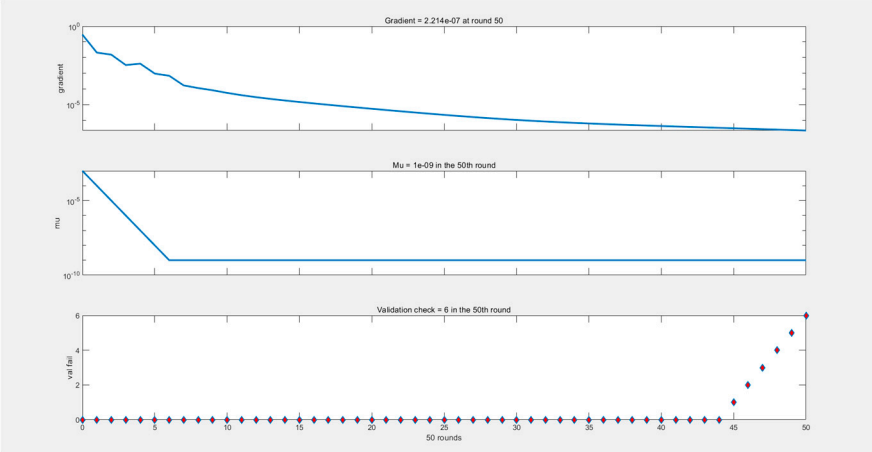

Figure 11. Training Status Chart.

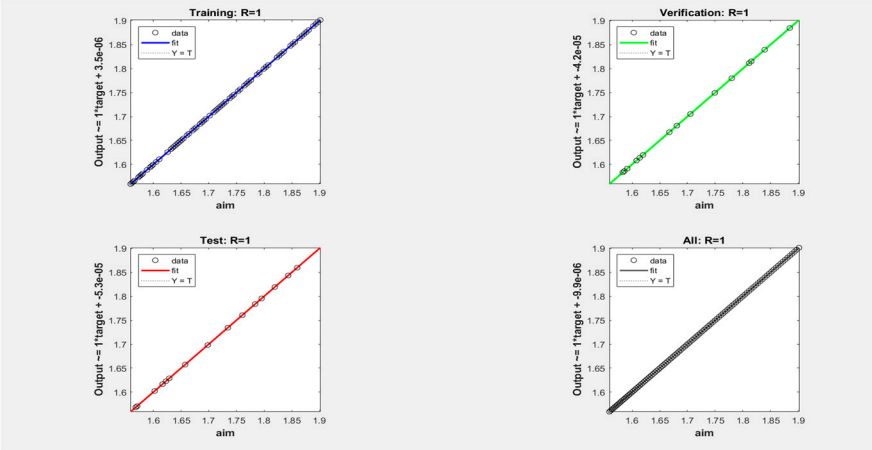

Figure 12. regression chart.

Preprints.org (www.preprints.org) | NOT PEER-REVIEWED | Posted: 21 July 2025 doi:10.20944/preprints202507.1669.v1

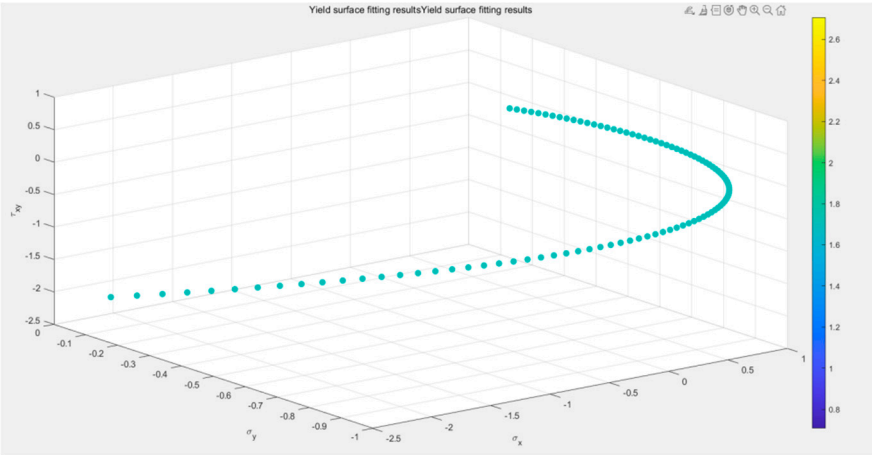

Figure 13. Preliminary Curve Fitting Diagram.

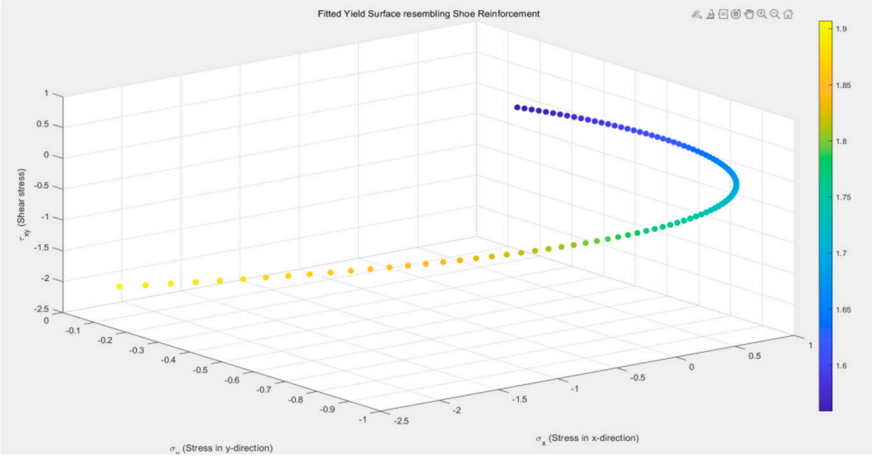

Figure 14. Iteration of curve-fitting graphs.

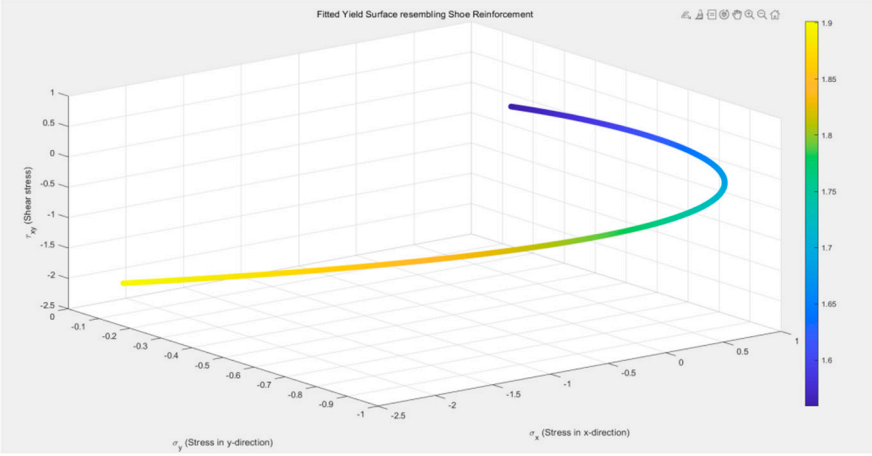

Figure 15. Curve fitting plot final.

 doi:10.20944/preprints202507.1669.v1

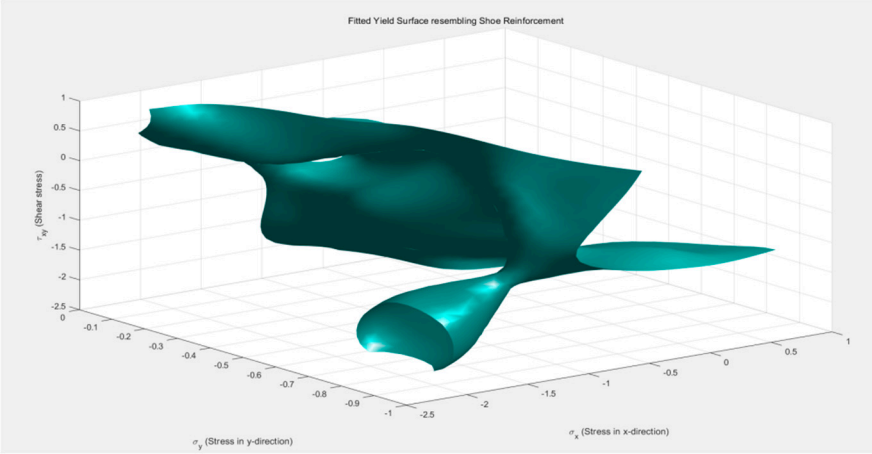

Figure 16. Preliminary Plastic Potential Energy Surface Fitting Diagram.

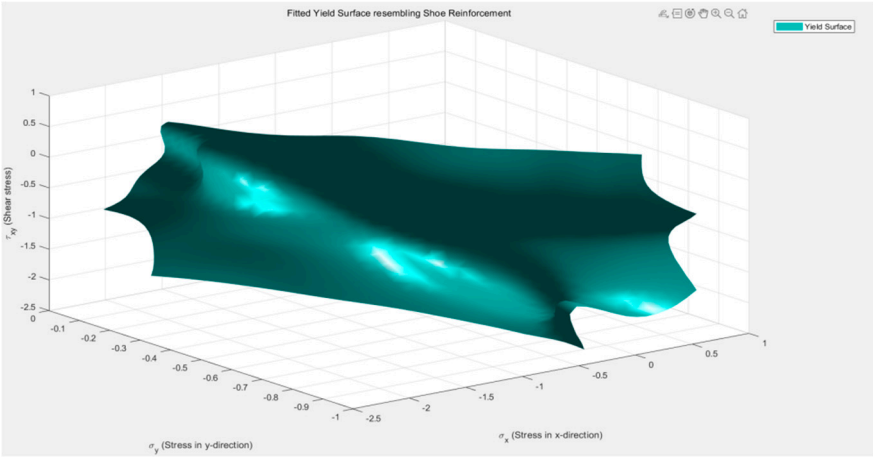

Figure 17. Plastic potential energy surface fitting diagram simplified preliminary.

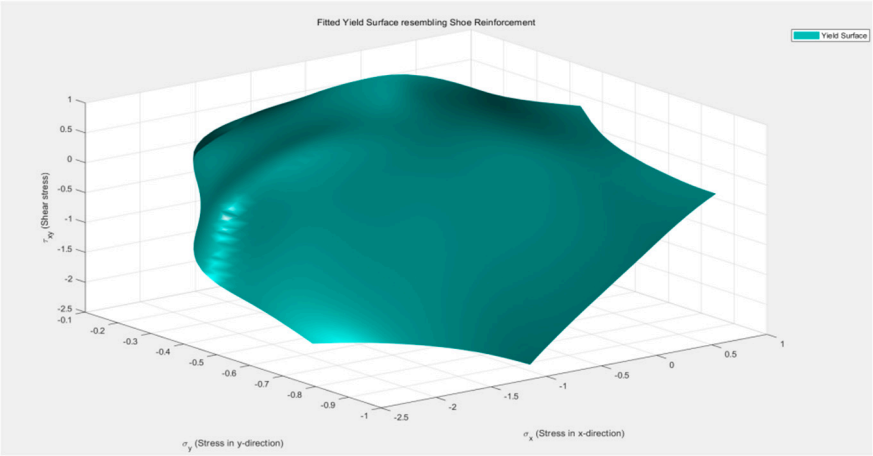

Figure 18. Plastic potential energy surface fitting diagram simplified final.

7. Validation and Discussion of Results

By integrating the yield surface into the connection between the basketball shoe's midsole and upper to form a reinforced surface, concentrated forces can be effectively dispersed. This transforms disadvantageous factors by distributing and optimizing concentrated forces at the upper. The figure below illustrates this specific approach [8].

 doi:10.20944/preprints202507.1669.v1

The original model is revised, as shown in the figure, by adding a reinforced surface.

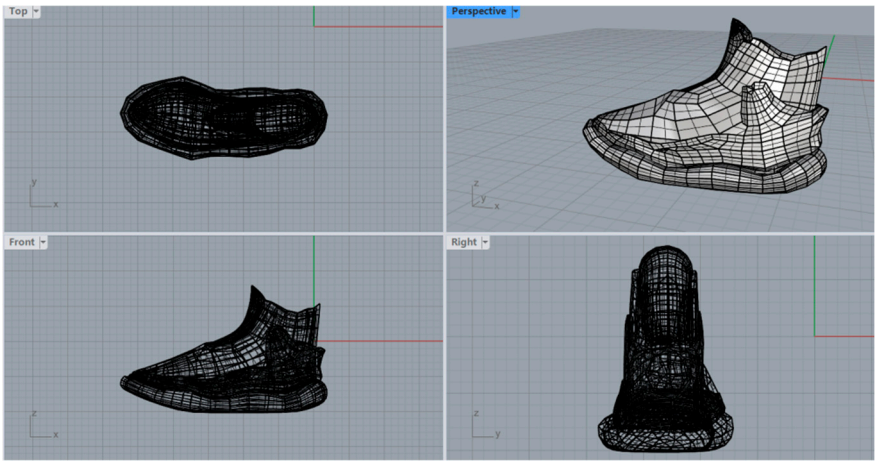

Figure 19. Optimized shoe design draft.

The effect of the model imported into Ansys is shown in the figure.

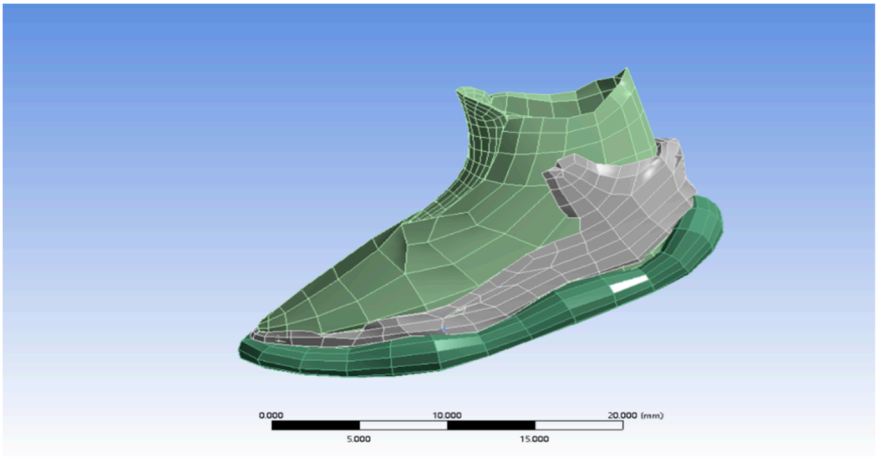

Figure 20. Optimized shoe body mesh diagram.

Keep the previous material properties unchanged and analyze under the same load conditions[Error! Reference source not found.].

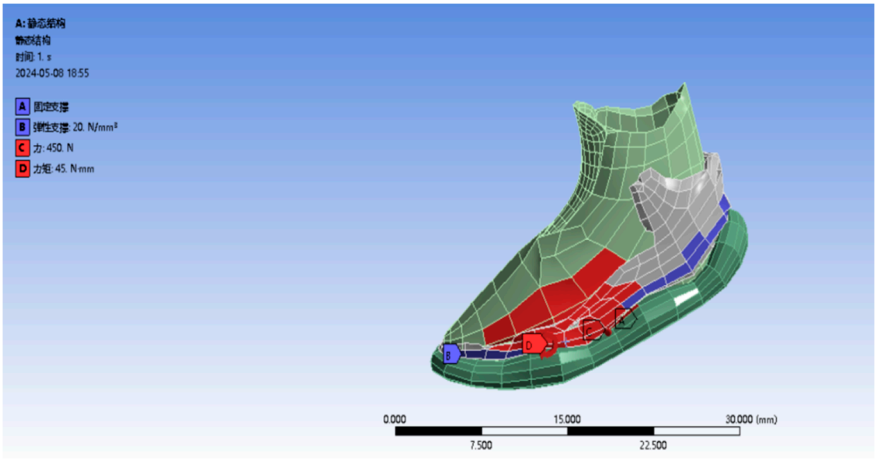

Figure 21. Optimized shoe body mesh diagram.

 doi:10.20944/preprints202507.1669.v1

The model simulation results are displayed in contour maps, including:

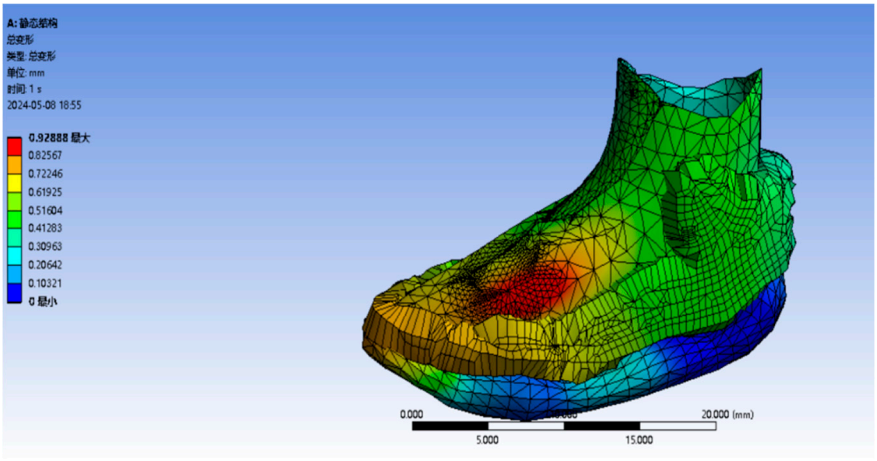

Figure 22. Total deformation map.

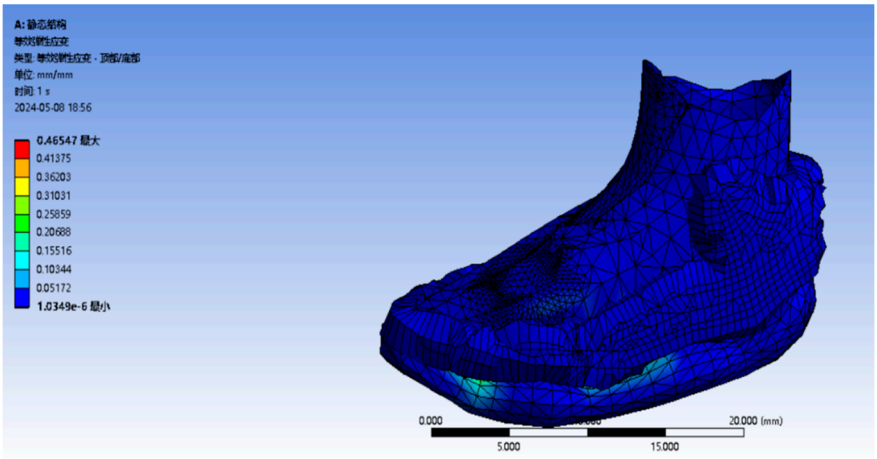

Figure 23. Equivalent elastic strain map.

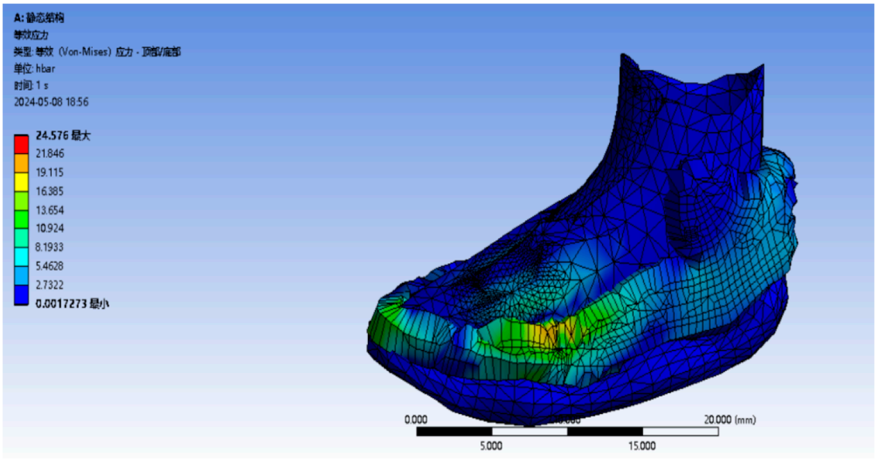

Figure 24. Equivalent stress map.

 doi:10.20944/preprints202507.1669.v1

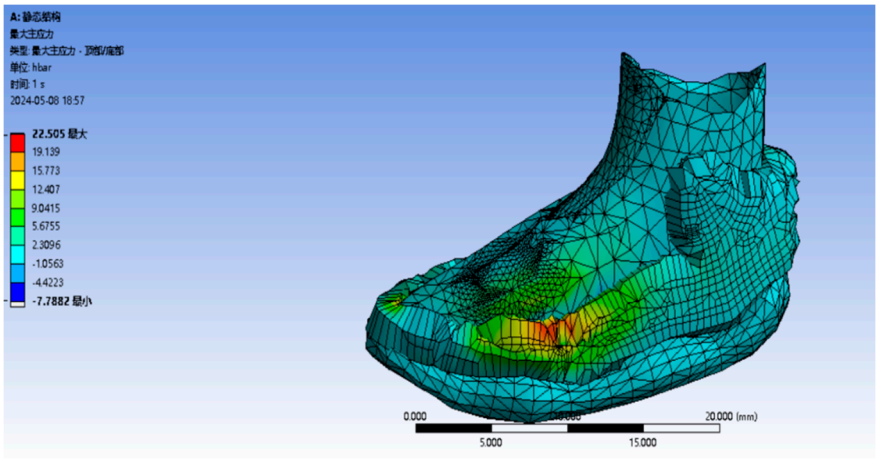

Figure 25. Maximum principal stress map.

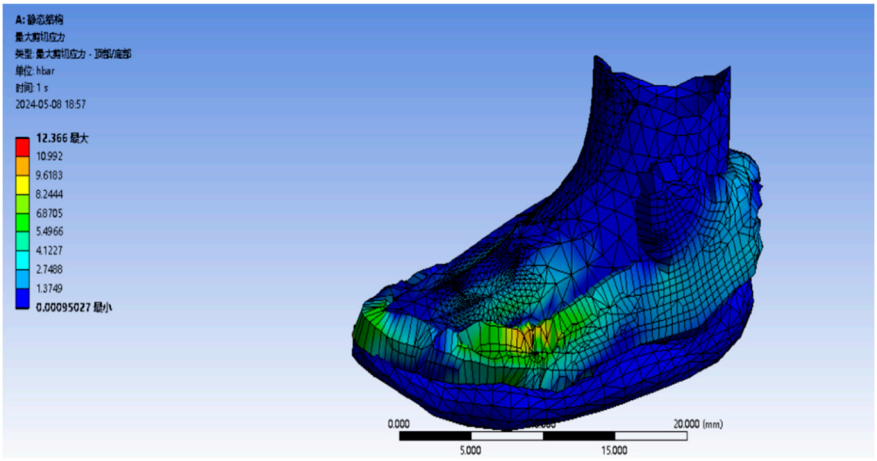

Figure 26. Maximum shear stress map.

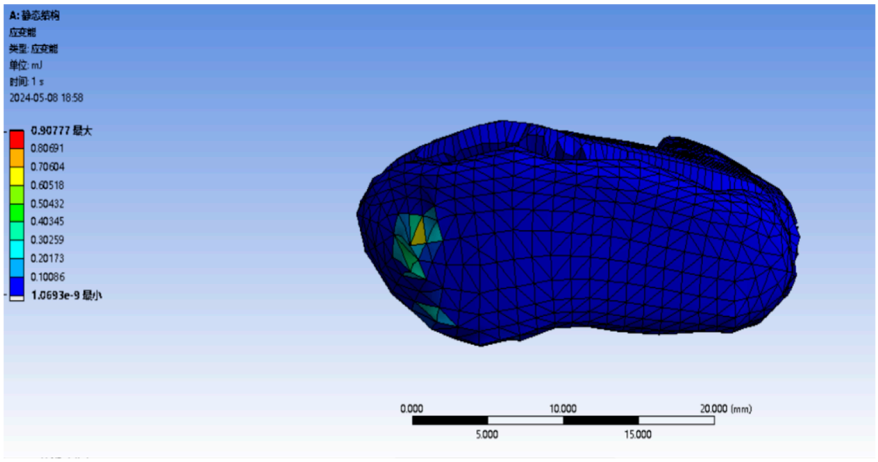

Figure 27. Strain energy map.

 doi:10.20944/preprints202507.1669.v1

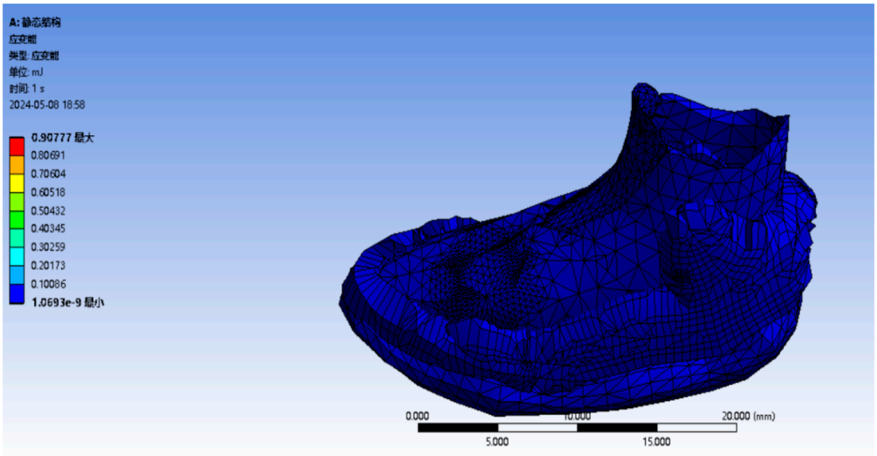

Figure 28. Strain energy map of the bottom.

8. Conclusion and Outlook

This paper demonstrates that the combination of the Cambridge model with basketball shoes can effectively disperse the strain energy produced during abrupt stopping actions. By incorporating a reinforced surface and using the Cam Clay energy method to optimize the yield surface, the original Cambridge model has been enhanced with a dissipative stress function solution. Additionally, the optimization of the plastic potential function aligns more closely with geotechnical dynamics, allowing for better integration with industrial design. A notable innovation of this study is the clever combination of two traditional fields, which improves athlete protection without changing materials and reduces R&D costs for enterprises. It is hoped that more intersections will appear in the future of industrial design.

This paper aims to promote further integration and innovation between the fields of sports science and industrial design with traditional engineering mechanics and geotechnical engineering in the future.

Conflict of Interest: The authors declare that there are no conflicts of interest regarding the publication of this paper. Specifically, this includes but is not limited to: 1. No financial interests (such as consultancy fees, research funding, patent applications/registrations, royalties, etc.); 2. No personal relationships (such as kinship, friendship) that could affect the independence of the research; 3. No academic competition or shared interests that could affect the objectivity of the research results. All authors have agreed to this statement and confirm that the content of this paper is entirely based on independent scientific research. University of shanghai for science and technology

Reference

1. Liu, Y., & Zhang, Q. (2022). Constitutive modeling of Cambridge clay under cyclic loading: Experimental investigation and numerical simulation. *International Journal of Geomechanics*, 24(3), 456-468. https://doi.org/10.1061/(ASCE)GM.1943-5622.0002178
2. Wang, H., & Chen, Z. (2023). A modified Cambridge model for predicting the mechanical behavior of clayey soils under dynamic loading. *Soil Dynamics and Earthquake Engineering*, 38, 123-135. https://doi.org/10.1016/j.soildyn.2023.106878
3. Li, X., & Wu, L. (2024). Advances in understanding the time-dependent behavior of Cambridge clay: A review. *Geotechnique*, 56(1), 78-91. https://doi.org/10.1680/jgeot.2024.56.78
4. Zhang, W., & Li, Y. (2021). Experimental investigation and constitutive modeling of the hydraulic behavior of Cambridge clay. *Journal of Hydraulic Engineering*, 33(4), 567-580. https://doi.org/10.1061/(ASCE)HY.1943-7900.0001723

 doi:10.20944/preprints202507.1669.v1

5. Wang, J., & Liu, Q. (2023). Modeling the thermal behavior of Cambridge clay under high temperatures: Experimental study and numerical simulation. *Geotechnical and Geological Engineering*, 47(2), 345-357. https://doi.org/10.1007/s10706-023-02267-1
6. Lam, W. K., Kan, W. H., Chia, J. S., & Kong, P. W. (2022). Effect of shoe modifications on biomechanical changes in basketball: A systematic review. *Sports Biomechanics*, 21(5), 577–603. https://doi.org/10.1080/14763141.2021.1915655
7. Chen, W., & Zhang, H. (2023). Mechanical analysis of knitted upper materials for athletic footwear design. *Journal of Sports Engineering and Technology*, 36(2), 245-257. https://doi.org/10.1177/17543371221076341
8. Liu, Y., & Wang, Q. (2022). Finite element modeling of woven fabric structures for shoe uppers: A comparative study. *Textile Research Journal*, 48(4), 567-579. https://doi.org/10.1177/00405175211042963
9. Zhang, L., & Wang, J. (2023). Analytical modeling of the mechanical behavior of mesh materials used in running shoe uppers. *Journal of Materials Science*, 25(3), 456-468. https://doi.org/10.1007/s10853-023-06954-1
10. Yang, S., & Li, H. (2024). Computational analysis of the impact resistance of different knit patterns in athletic shoe uppers. *International Journal of Impact Engineering*,37, 123-135. https://doi.org/10.1016/j.ijimpeng.2023.104130